Modern Research in Catalysis, 2015, 4, 1-12
Published Online January 2015 in SciRes. http://www.scirp.org/journal/mrc
http://dx.doi.org/10.4236/mrc.2015.41001

Effect of Tantalum Doping on TiO_2 Nanotube Arrays for Water-Splitting

Alfonso Pozio

ENEA, C.R. Casaccia, Via Anguillarese 301, 00123, S. Maria di Galeria, Rome, Italy
Email: alfonso.pozio@enea.it

Received 20 October 2014; revised 21 November 2014; accepted 20 December 2014

Abstract

This work is intended to define a new possible methodology for TiO_2 doping through the use of electrochemical deposition of tantalum directly on the titanium nanotubes obtained by a previous galvanostatic anodization treatment in an ethylene glycol solution. This method does not seem to cause any influence on the nanotube structure, showing final products with news and interesting features with respect to the unmodified sample. Together with a decrease in the band gap and flat band potential of the TiO_2 nanotubes, the tantalum doped specimen reports an increase of the photo conversion efficiency under UV light.

Keywords

Nanotube, TiO_2, Water Photoelectrolysis, Photoelectrode, OER

1. Introduction

The publication of the fundamental work of Gong *et al*. [1], in which the authors created the basis for the development of a new synthesis model for the titania nanotubes based on the anodic oxidation of a titanium foil in fluoride based solutions, opened the way to a new methodology able to combine a simplicity of preparation of the material with a complete control of physical characteristics of the nano-system [2]-[5]. Besides, being its particular geometric shape particularly appropriate for an application as photo-anode in water-photoelectrolysis [6], many studies have been directed towards this field, which have arrived to report elevated values of UV photoconversion efficiency for these nanosystems [7] [8]. In the meanwhile, a large range of different applications for this material has been discovered. In fact, for example, it is reported that the electrical resistance of the titania nanotubes was highly sensitive to the chemisorbed hydrogen molecules hydrogen sensing [9] [10], creating a new route in the hydrogen sensing research field [11] [12]. But, many other similar examples of the wide versatility of the TiO_2 nanotube arrays are available in literature, as the dye-sensitized solar cells [13]-[17], li-

How to cite this paper: Pozio, A. (2015) Effect of Tantalum Doping on TiO_2 Nanotube Arrays for Water-Splitting. *Modern Research in Catalysis*, **4**, 1-12. http://dx.doi.org/10.4236/mrc.2015.41001

thium batteries [18] and also in different biological and medical reasearches, like the osteoblast growth [19]-[22] or drug elution [23]-[25]. As regards the application of the TiO_2 nanotube arrays as photo-electrodes for water photoelectrolysis, it is important to emphasize that although many important results have been reached in this field, the commercialization of such nanosystems is still far because of the high band gap of titania, which limits the light adsorption only to limited UV region [6]. So, in order to shift the light adsoption to lower energy region, many researchers focused their attention on the doping of these nanostructures. Different approaches and techniques have been used to obtain an effective doping, using nitrogen [26]-[32], carbon [33]-[37] or boron [38] [39] as doping agents. The most common procedures reported in the literature can be roughly divided into three main categories: 1) modification of the components of the anodic bath, in order to incorporate the anionic dopants during the anodization growth [29] [40] [41]; 2) thermal annealing in controlled atmosphere, using gas like pure ammonia [42] [43], dry nitrogen [44], CO [33] or H_2S [45]; 3) ion implantation [27] [28]. Metal-doped semiconductors, including Ta-doped TiO_2, have been widely studied for improved physical and chemical properties owning to the significant effects of the metal ion dopants on their inner electronic and/or crystalline structures [46]. It was reported that dopants with a +5 valence, such as Ta, have an ionic radius similar to that of Ti^{4+} [47]. This dopant readily dissolves in the TiO_2 lattice by donating conductive electrons. Feng *et al*. [48] successfully prepared tantalum-doped TiO_2 nanowire arrays by a low-temperature hydrothermal method. In addition, Ta, N co-doped TiO_2 thin films in an anatase form were fabricated by means of a radio-frequency (RF) magnetron sputtering method [49]. In this work, we intended to describe an effect obtained by modifying the preparation of nanotubes, as proposed in previous works [8] [50], by a subsequent electro-deposition, in an organic solution containing Ta^{5+} ions, on the lattice of the titanium dioxide.

We have found that doped titania nanotube arrays own different features with respect to the starting undoped structure. The energy gap showed to be reduced and the levels of conduction and valence band be shifted. These changes produced an increase of the photo-conversion efficiency. We retain that this methodology, if optimized and deepened, could open a new route to a best effective doping of the titania nanotube arrays.

2. Experimental

2.1. Materials and Photo-Electrode Preparation

A small disk of commercially pure grade-3 titanium (Titania, Italy) has been used as substrate for the nanotube growth. The circular sample had a diameter of 15 mm with a thickness of 0.5 mm, and was arranged to show an active circular area of 1 cm^2. The un-modified sample (TiO_2/Ti) was prepared with the methodology previously developed in different articles [8] [50]. Briefly, after 3 min. pickling in a HF (Carlo Erba)/HNO_3 (Carlo Erba) solution made by a volumetric ratio of 1:3 and diluted in deionised water until to 100 ml, the titanium disks have been set in a three-electrode cell containing a 1 M KOH solution (Carlo Erba) and subjected to a prefixed and optimized density current (1 $mA \cdot cm^{-2}$) generated by a potentiostat/galvanostat (Solartron 1286) for 3 min. The counter-electrode was a platinum sheet, while the reference was a standard calomel electrode (SCE). The anodic growth of the nanotube arrays has been obtained in a two-electrode cell with a platinum counter electrode, using a glycol ethylene (Ashland) solution with 1 %wt. H_2O and 0.2 %wt. NH_4F and applying 60 V for 3 h by means of a potenziostat/galvanostat PS251-2 (Aldrich). The current has been measured with a Keithley 2000 multimeter and been acquired with a Madge-Tech Volt101 digital recorder placed in series with a calibrated resistance (300 Ω) Leeds and Northrup (**Figure 1**).

After the anodization, the sample was washed in glycol ethylene and left overnight in a dry room. In order to transform amorphous TiO_2 nanotubes obtained by anodic growth into the anatase phase, which shows a higher photosensibility, after a pre-heat treatment at 90˚C in vacuum for 3 hours, the sample has been placed in a tubular furnace (Lenton) for 1 h at 580˚C with a slope of 1˚C·min^{-1} in air.

After the physical and electrochemical characterizations, the same TiO_2/Ti sample was doped with tantalum in order to obtaining a modified nanotube arrays Ta-TiO_2/Ti. Using the **Figure 1** system, tantalum's atoms have been electro-deposited on the TiO_2/Ti specimen but, in this case, the TiO_2/Ti has been placed as a cathode while the anode counter-electrode was a tantalum's sheet pure (5 cm^2). The electrodes were placed at a distance of 1 cm in a glycol ethylene (Ashland) solution with 1 %wt. H_2O and 0.2 %wt. NH_4F and tantalum anode was anodized at 0.1 mA for 10 min. After the deposition the sample was washed in distilled and left overnight in a dry room. Then, the doped sample has underwent again the physical and electrochemical characterizations in order to evaluate the difference.

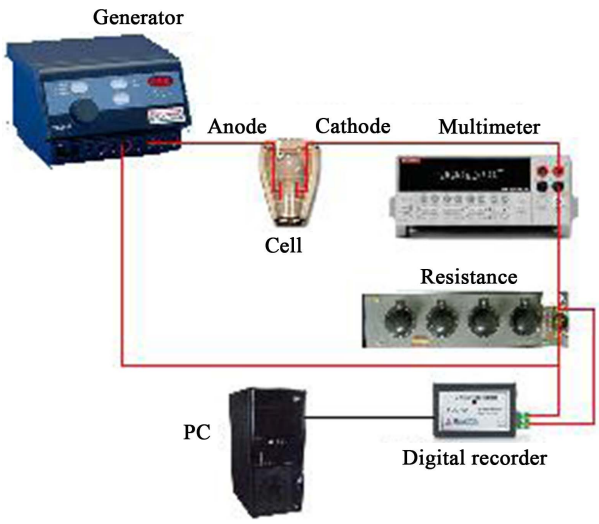

Figure 1. Scheme of anodization system.

2.2. Surface Analysis

The material structure was investigated with a Rigaku Miniflex diffractometer. The patterns were obtained using a Cu Kα radiation from a rotating anode source operating at 30 kV and 15 mA. The specimens were scanned at 0.02˚ s^{-1} in the continuous scan mode over the 2θ range 20˚ - 120˚.

2.3. Electrochemical Measurements

The electrochemical measurements were performed using a system similar to the one described by Shankar *et al.* [7]. Briefly, it is made of a pyrex cell with a 1.5 cm diameter quartz window, where the light, emitted by UV (Ultravitalux Osram) lamp placed at distances of 4.5 cm. The source has a spectrum with peak intensity in the UVA region at 360, 400 nm and the UV intensity, which is measured on the sample by a photo-Radiometer HD2302.0 (Delta OHM) over the spectral range 220 - 400 nm, is 24 $W \cdot m^{-2}$. Along the optical path to the cell, a lens was interposed in order to collimate the radiation of the light source. The active surface of the sample (1 cm^2) was immersed in a KOH 1 M solution and placed at 0.5 cm from the quartz window (**Figure 2**). Photocurrents and "open circuit potential" (OCP) measurements were made via a potentiostat 1287 (Solartron). The potentiodynamic were performed with a scan rate of 20 $mV \cdot s^{-1}$ in the range of potential −1.23 ÷ 1.70 V vs. NHE in conditions of presence and absence of UV. The OCP measures were recorded in the presence and absence of UV. Impedance measurements were performed in the same cell by means of a generator of frequency response 1260 (Solartron) in the range of 65 kHz ÷ 1 Hz with a sinusoidal signal of amplitude 10 mV. In particular the charging layer capacity (CSC) of the interface electrode/electrolyte was measured at a frequency of 15 kHz, applying a scanning potential of 1 $mV \cdot s^{-1}$ between −1 ÷ 2.25 V vs. NHE and with an alternating component of 10 mV in order to obtain the Mott-Schottky plot.

2.4. UV-Vis Absoption Spectra

The diffuse reflectance spectrum of the TiO_2 samples was obtained using a Lambda 9 spectrophotometer equipped with an integrating sphere. The reflectance data was converted to the absorption coefficient $F(R_\infty)$ values according to the Kubelka-Munk equation [51] [52]:

$$F(R_\infty) = \frac{(1-R_\infty)^2}{2R_\infty} \tag{1}$$

The absorption coefficient $F(R_\infty)$ and the bandgap E_g are related through the equation [53]:

$$\left[F(R_\infty)\cdot h\nu\right]^S = h\nu - E_g \tag{2}$$

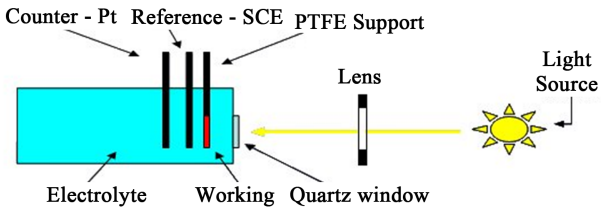

Figure 2. Experimental setup.

where v is the frequency, h is the Planck's constant, and $S = 0.5$ for indirect bandgap material [6]. In this way, the plotting of $\left[F\left(R_\infty\right)\cdot h\nu\right]^{0.5}$ vs. $h\nu$, the so-called Tauc plot, gives the possibility to obtain the optical bandgap by dropping a line from the maximum slope of the curve to the x-axis [54]-[57].

3. Results and Discussion

3.1. Ta Doped TiO_2 Nanotube Arrays

The doping of the TiO_2/Ti specimen is based on the evidence that, in this experimental condition, the tantalum sheet undergoes an anodization (Equation (3)) and an etching process (Equation (4)) similar to that observed for the titanium with dissolution of TaF_6^- specie [58] [59]:

$$2Ta + 5H_2O \Rightarrow Ta_2O_5 + 10H^+ + 10e^- \tag{3}$$

$$Ta_2O_5 + 12F^- + 10H^+ \rightarrow 2TaF_6^- + 5H_2O \tag{4}$$

In this condition, we have a continuous Ta^{5+} ion release in the glycol solution that can be used as doping agent for the TiO_2 nanotubes cathode.

It is known that, under cathodic polarization metal oxides can show significant cation in-diffusion, combined with reduction of the oxide [60]. This process is accompanied by alterations in the electronic structure of the oxide (e.g., incorporation of additional states within the band gap that change conductivity and optical properties of the material). In our case, the process could be ascribed as:

$$Ti^{IV}O_2 + Ta^{5+} \rightarrow Ti^{III}O_2Ta \tag{5}$$

For many oxides and applied conditions this process is electrochemically reversible. Such intercalating ion uptake and release is applied for example in rechargeable batteries and switchable electrochromic devices. Obviously, the main cathode reaction is the hydrogen evolution (HER) but very few tantalum atoms can be electrodeposited onto the nanotubes surface undergoing oxidation (Equation (3)) with a mechanism like that showed in **Figure 3**.

Following this hypothesis, in TiO_2 lattice, under the F^- etching action, titanium ions and oxide ions can deviate from their normal lattice positions, leave titanium vacancy and oxide vacancy behind. The dopant Ta, which has a 5^+ valence and an ionic radius similar to that of Ti^{4+}, acts as a donor when dissolved into the TiO_2 lattice. So, the dissolution of Ta into the titanium oxide grains can contributes to the generation of electrons and holes for conduction which give rise to an increase of the semi-conducting behaviour [47] [61].

The XRD pattern of nanotube TiO_2/Ti, obtained through electrosynthesis route, is depicted in **Figure 4**. From comparison with the Ta-TiO_2/Ti substrate pattern (black trace), no difference can be noted and all features typical of the titanium metal and TiO_2 are observed. Particularly, a few peaks, ascribable to titanium oxide material anatase and rutilo can be recognized [62] [63]. The results indicate that Ta doping does not introduce changes in the TiO_2 structure.

3.2. Analysis of the Absorbance Spectra

The diffuse absorbance spectra of the two samples, obtained by the Kubelka-Munk equation, are showed in **Figure 5**. Both the samples show the main absorbance in the UV range of 300 - 350 nm, but the TiO_2/Ti sample owns a better behavior in this part of the spectrum. Instead, the Ta-TiO_2/Ti specimen shows an increase in the low UV region, starting from a wavelength of 380 nm.

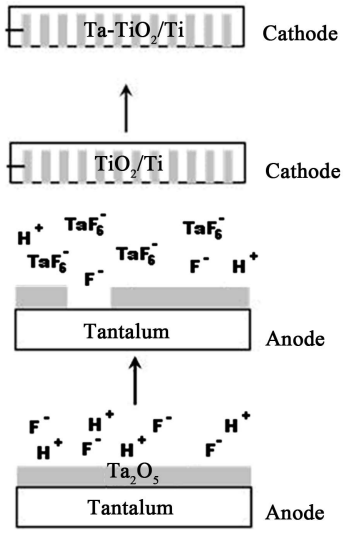

Figure 3. Schematic representation of the reaction leading to the Ta doping.

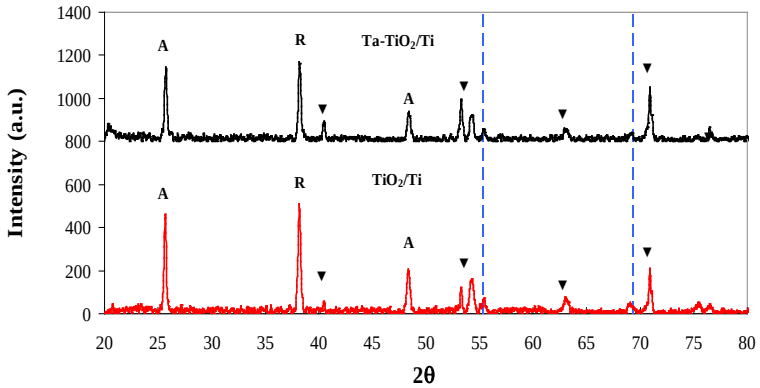

Figure 4. XRD pattern of nanotube TiO_2/Ti and Ta-TiO_2/Ti obtained through electrosynthesis route; (A) anatase, (R) rutilo, (▼) titanium. The dashed lines indicate the Ta position [63].

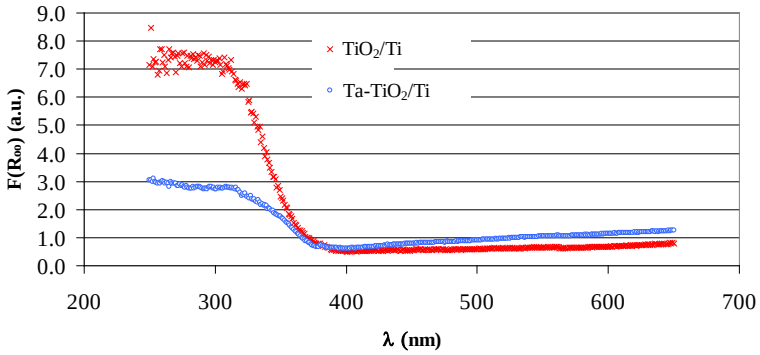

Figure 5. Diffuse reflectance spectra of the TiO_2/Ti (×) and Ta-TiO_2/Ti (○) according to the Kubelka-Munk equation.

The band gaps of the two samples are calculated using the Tauc plot (**Figure 6**), as previously described. The result of this operation shows a decrease of the Ta-TiO_2/Ti band gap of about 0.204 eV with respect the normal titania nanotube arrays.

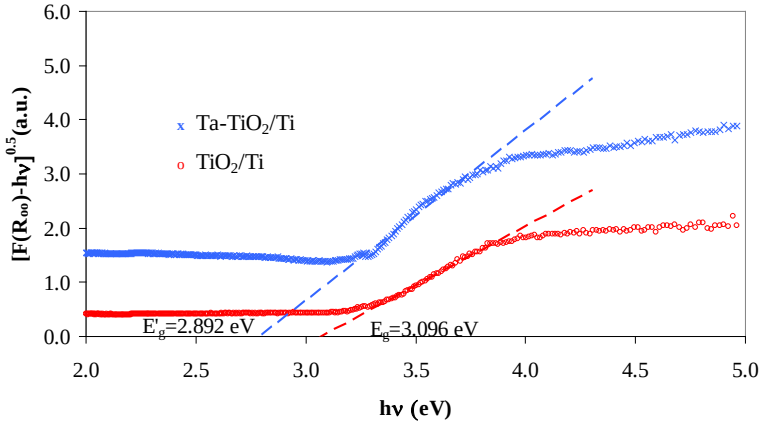

Figure 6. Transformed Kubelka-Munk function vs. energy of excitation source for TiO_2/Ti (×) and Ta-TiO_2/Ti (○).

3.3. Analysis of the Photo-Electrochemical Performance

Figure 7 shows the open circuit potential (E_{ocv}) for TiO_2/Ti and Ta-TiO_2/Ti with UV on and off. When applying the UV, E_{ocv} decreases sharply and it reaches a steady state at a lower potential. After the switching off the light source, E_{ocv} increases rapidly in the first seconds and then slowly until to a new steady state level. In UV on condition, the doped electrode shows an E_{ocv} of −0.68 V vs NHE while the un-doped one −0.57 V. The decrease of photo-potential indicates a clear effect on the degree of band bending for the doped n-type metal oxide semiconductor.

Figure 8 shows the curves of photo-current and photo-electrochemical performance of TiO_2/Ti and Ta-TiO_2/Ti. The photo-conversion efficiency η, which is the light energy to chemical energy conversion efficiency, is calculated as [7]:

$$\eta(\%) = i_{ph}\frac{\left[E_{rev}^{o} - \left|E_{app}\right|\right]}{J_o}\times 100 \tag{6}$$

where i_{ph} is the photocurrent density (mA·cm^{-2}), $i_{ph}E_{rev}^{0}$ is the total power output, $i_{ph}\left|E_{app}\right|$ is the electrical power input and J_0 is the power density of incident light, which is 2.4 mW·cm^{-2}. E_{rev}^{0} is the standard reversible potential of 1.23 V/NHE. The applied potential can be calculated:

$$E_{app} = E_{meas} - E_{ocv} \tag{7}$$

where E_{meas} is the electrode potential (versus NHE) of the working electrode, at which photocurrent was measured under illumination, E_{ocv} is the electrode potential (versus NHE) of the same working electrode at open circuit conditions under the same illumination and in the same electrolyte.

After doping, the efficiency of photo-electrochemical rose from 8% to 12% with an increase in photocatalytic activity by 49%. The onset photo potential for the discharge of water E'' moves to more negative values from −0.68 to −0.84 V vs. NHE. In contrast, the potential onset of E' remains almost unchanged at approx. 0.77 V vs. NHE. At the same time, however, it has a supplementary reduction of the catalytic activity of 40% shown by the reduction of current for higher potential to 1.25 V.

The flat band potential E_{fb} has been determined for both electrodes from the photocurrent measurements applying the equation [64] [65].

$$i_{ph}^{2} = \left(\frac{2\varepsilon_r\varepsilon_0 e\alpha J_o}{N_D}\right)\left(E_{meas} - E_{fb}\right) \tag{8}$$

where N_D denotes the donor density, ε_r the relative dielectric constant of the TiO_2 anodic film (55) [66], ε_0, the vacuum permittivity (8.86 × 10^{-14} F·cm^{-1}), e the charge of an electron (1.602 × 10^{-19} C), and α the light absorption coefficient for the material.

The E_{fb} calculated in the **Figure 9** as the intercept with the abscissa, decrease for Ta doped of about 22% from −0.56 to −0.72 V vs. NHE thus indicating a possible change in the semiconductor electronic structure.

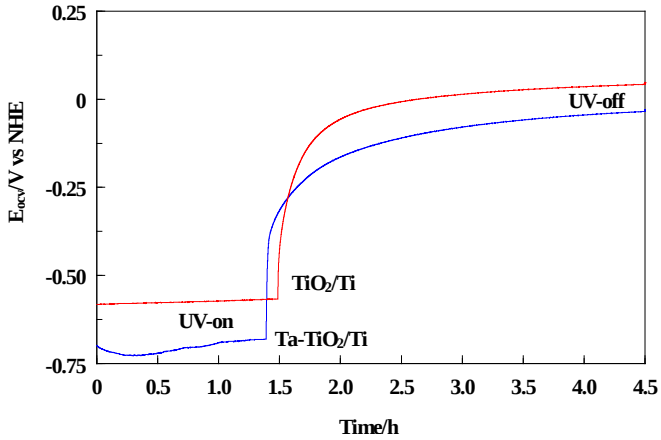

Figure 7. Open circuit potential at UV on and off for TiO_2/Ti (red) and Ta-TiO_2/Ti (blue).

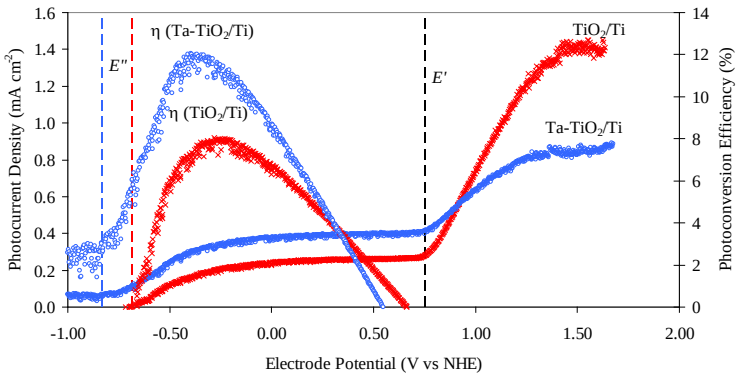

Figure 8. UV photocurrent density and efficiency vs. voltage for TiO2/Ti (x) and Ta-TiO2/Ti (o).

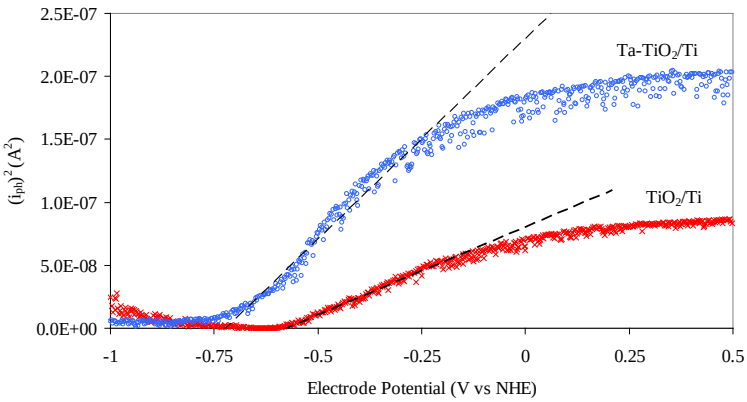

Figure 9. Square photocurrent vs. electrode potential for TiO_2/Ti (×) and Ta-TiO_2/Ti (○).

The slope of the so-called Mott-Schottky plots allows calculation of the donor density [67]-[70]. The change of the n-semiconductor doping density N_D can be estimated using the Mott-Schottky relationship in the linear part of diagram by the equation [66] [67]:

$$N_D = \frac{2}{ke\varepsilon_r\varepsilon_0} \tag{9}$$

where k is the slope of $(1/C_{sc})^2$ vs. electrode potential plot. **Figure 10** shows the Mott-Schottky plot for TiO_2/Ti and Ta-TiO_2/Ti, evidencing a clear decrease of the k slope after the Ta doping with a calculated N_D increase from 1.3×10^{27} m^{-3} to 2.4×10^{27} m^{-3}.

All the photo-electrochemical characteristic of TiO_2/Ti and Ta-TiO_2/Ti are summarized in **Table 1**.

In considering light receptor electrodes for photo-electrochemical cells an important criterion is the absolute position of the valence (*VB*) and conduction bands (*CB*). In fact, fast electron transfer across the electrolyte semiconductor interface occurs when the appropriate band overlaps the redox level of the electrolyte. This is important since recombination of the photo-generated electron-hole pair competes with the electron transfer, and thus these relative rates influence quantum efficiency. The absolute position of the bands effectively controls the degree of band bending, E_B, since the surface Fermi level, E_F, for the heavily doped n-type metal oxide semiconductor approximately coincides with the *CB* level. The value of E_B is generally taken as the difference between E_F and the "Fermi level" of the electrolyte which is taken as the redox potential, E_{redox} for the reaction occurring at the photo-electrode [69]:

$$E_B = E_F - E_{F-Redox} \tag{10}$$

for water oxidation in alkaline media (Equation (9)) and for TiO_2/Ti n-type semiconductor photo-electrodes E_{redox} is the $O_2|OH^-$ potential:

$$2h^+ + 2OH^- \rightarrow 1/2\,O_{2(g)} + H_2O_{(l)} \quad \left(E^\circ = 0.401\text{ V vs. NHE}\right). \tag{11}$$

The maximum open-circuit photo-potential is E_B and if it exceeds 1.23 V, then it is possible to run water splitting without any other energy source other than the light. To the extent that E_B falls short of 1.23 V (plus any required overvoltage) one requires an additional energy input assisting the effect; an applied potential, V_{app}, must be supplied to provide the difference. Since $E_F = E_{CB}$ for the materials of interest here, we can conclude from this discussion that the *CB* position must be 1.23 V above the $O_2|OH^-$. This analysis evidence that Ta doping shift the absolute position of the valence and conduction band so increasing the E_B value and reducing the overvoltage required for water splitting.

The increase of donor density justify the shift of energy levels. The position of the Fermi level lies between the valance and conduction bands, it is dependent on the electron accumulation within the semiconductor particles. So, the main Ta doping effect is to accumulate more electrons/holes within the semiconductor structure and following the band gap excitation, the Fermi level becomes more negative and shifts closer to the conduction-band edge [71].

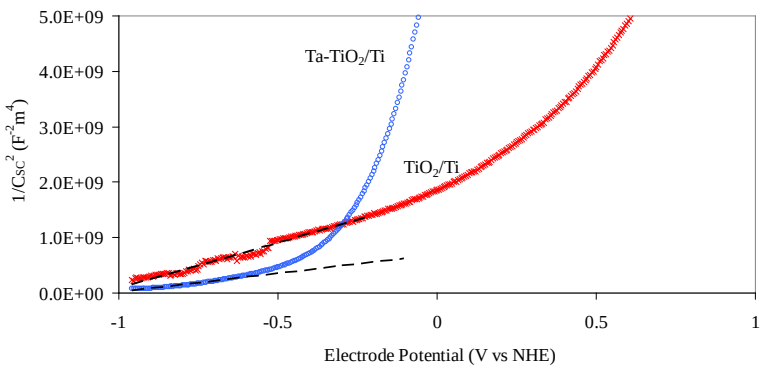

Figure 10. Mott-Schottky plots for TiO_2/Ti (×) and Ta-TiO_2/Ti (○).

Table 1. Photo-electrochemical characteristic of TiO_2/Ti and Ta-TiO_2/Ti anodes.

Sample	E_{OCV} V#	η %	i_{ph}* μA cm^{-2}	$E_{FB} \approx E_{CB}$ V# (eV)	E_{VB} V# (eV)	E_B V# (eV)	N_D m^{-3}
TiO_2/Ti	−0.57	8.03	285	−0.59 (−4.01)	2.28 (6.88)	−0.99	1.3×10^{27}
Ta-TiO_2/Ti	−0.68	12.04	446	−0.72 (−3.88)	2.07 (6.67)	−1.12	2.4×10^{27}

#V vs NHE; *measured at 0.241 V vs. NHE.

4. Conclusion

In this work, we have reported a preliminary study for a new possible doping route for anodic titania nanotubes. This methodology, yet to be improved and optimized, shows as a first positive feature the fact that the presence of a Ta ions into the TiO_2 nanotubes can produce relevant changes in the electronic structure. Besides, this technique leads to a decrease in the TiO_2 band gap and an improvement of the ability of the titania nanotubes to use UV radiations of lower energy.

Acknowledgements

We would thank Dr. Alberto Mittiga of ENEA Utrinn-FVC for the Absorption Spectra measurements.

References

[1] Gong, A., Grimes, C.A., Varghese, O.K., Hu, W., Singh, R.S., Chen, Z. and Dickey, E.C. (2001) Titanium Oxide Nanotube Arrays Prepared by Anodic Oxidation. *Journal of Materials Research*, **16**, 3331-3334. http://dx.doi.org/10.1557/JMR.2001.0457

[2] Mor, G.K., Varghese, O.K., Paulose, M., Mukherjee, N. and Grimes, C.A. (2003) Fabrication of Tapered, Conical-Shaped Titania Nanotubes. *Journal of Materials Research*, **18**, 2588-2593. http://dx.doi.org/10.1557/JMR.2003.0362

[3] Cai, Q., Paulose, M., Varghese, O.K. and Grimes, C.A. (2005) The Effect of Electrolyte Composition on the Fabrication of Self-Organized Titanium Oxide Nanotube Arrays by Anodic Oxidation. *Journal of Materials Research*, **20**, 230-236. http://dx.doi.org/10.1557/JMR.2005.0020

[4] Kontos, A.G., Kontos, A.I., Tsoulkleris, D.S., Likodimos, V., Kunze, J., Schmuki, P. and Falaras, P. (2009) Photo-Induced Effects on Self-Organized TiO_2 Nanotube Arrays: The Influence of Surface Morphology. *Nanotechnology*, **20**, 045603 (1-9). http://dx.doi.org/10.1088/0957-4484/20/4/045603

[5] Mor, G.K., Shankar, K., Paulose, M., Varghese, O.K. and Grimes, C.A. (2005) Enhanced Photocleavage of Water Using Titania Nanotube Arrays. *Nano Letters*, **5**, 191-195. http://dx.doi.org/10.1021/nl048301k

[6] Grimes, C.A., Varghese, O.K. and Ranjan, S. (2008) The Solar Hydrogen Generation by Water Photoelectrolysis. Springer, New York.

[7] Shankar, K., Mor, G.K., Prakasam, H.E., Yoriya, S., Paulose, M., Varghese, O.K. and Grimes, C.A. (2007) Highly-Ordered TiO_2 Nanotube Arrays up to 220 µm in Length: Use in Water Photoelectrolysis and Dye-Sensitized Solar Cells. *Nanotechnology*, **18**, 065707 (1-11). http://dx.doi.org/10.1088/0957-4484/18/6/065707

[8] Mura, F., Masci, A., Pasquali, M. and Pozio, A. (2010) Stable TiO_2 Nanotube Arrays with High UV Photoconversion Efficiency. *Electrochimica Acta*, **55**, 2246-2251. http://dx.doi.org/10.1016/j.electacta.2009.11.060

[9] Varghese, O.K., Gong, D., Paulose, M., Ong, K.G., Dickey, E.C. and Grimes, C.A. (2003) Extreme Changes in the Electrical Resistance of Titania Nanotubes with Hydrogen Exposure. *Advanced Materials*, **15**, 624-627. http://dx.doi.org/10.1002/adma.200304586

[10] Varghese, O.K., Gong, D., Paulose, M., Ong, K.G. and Grimes, C.A. (2003) Hydrogen Sensing Using Titania Nanotubes. *Sens. Actuators B*, **93**, 338-344. http://dx.doi.org/10.1016/S0925-4005(03)00222-3

[11] Chen, Q., Xu, D., Wu, Z. and Liu, Z. (2008) Free-Standing TiO_2 Nanotube Arrays Made by Anodic Oxidation and Ultrasonic Splitting. *Nanotechnology*, **19**, 365708, 5 p.

[12] Sennik, E., Colak, Z., Kilinc, N. and Ozturk, Z.Z. (2010) Synthesis of Highly-Ordered TiO_2 Nanotubes for a Hydrogen Sensor. *International Journal of Hydrogen Energy*, **35**, 4420-4427. http://dx.doi.org/10.1016/j.ijhydene.2010.01.100

[13] Mor, G.K., Shankar, K., Paulose, M., Varghese, O.K. and Grimes, C.A. (2007) High Efficiency Double Heterojunction Polymer Photovoltaic Cells Using Highly Ordered TiO_2 Nanotube Arrays. *Applied Physics Letters*, **91**, 152111(pp3). http://dx.doi.org/10.1063/1.2799257

[14] Mor, G.K., Basham, J., Paulose, M., Kim, S., Varghese, O.K., Vaish, A., Yoriya, S. and Grimes, C.A. (2010) High-Efficiency Förster Resonance Energy Transfer in Solid-State Dye Sensitized Solar Cells. *Nano Letters*, **10**, 2387-2394. http://dx.doi.org/10.1021/nl100415q

[15] Wang, Y., Yang, H., Liu, Y., Wang, H., Shen, H., Yan, J. and Xu, H.M. (2010) The Use of Ti Meshes with Self-Organized TiO_2 Nanotubes as Photoanodes of All-Ti Dye-Sensitized Solar Cells. *Progress in Photovoltaics*: *Research and Applications*, **18**, 285-290.

[16] Alivov, Y. and Fan, Z.Y. (2010) Dye-Sensitized Solar Cells Using TiO_2 Nanoparticles Transformed from Nanotube Arrays. *Journal of Materials Science*, **45**, 2902-2906. http://dx.doi.org/10.1007/s10853-010-4281-2

[17] Liu, Z. and Misra, M. (2010) Bifacial Dye-Sensitized Solar Cells Based on Vertically Oriented TiO_2 Nanotube Arrays. *Nanotechnology*, **21**, 125703, 4 p.

[18] Fang, D., Liu, S.Q., Chen, R.Y., Huang, K.L., Li, J.S., Yu, C. and Qin, D.Y. (2008) Fabrication and Characterization of Highly Ordered Porous Anodic Titania on Titanium Substrate. *Journal of Inorganic Materials*, **23**, 647-651. http://dx.doi.org/10.3724/SP.J.1077.2008.00647

[19] Oh, S.H., Finones, R.R., Daraio, C., Chen, L.H. and Jin, S. (2005) Growth of Nano-Scale Hydroxyapatite Using Chemically Treated Titanium Oxide Nanotubes. *Biomaterials*, **26**, 4938-4943. http://dx.doi.org/10.1016/j.biomaterials.2005.01.048

[20] Oh, S.H. and Jin, S. (2006) Titanium Oxide Nanotubes with Controlled Morphology for Enhanced Bone Growth. *Materials Science and Engineering*: *C*, **26**, 1301-1306. http://dx.doi.org/10.1016/j.msec.2005.08.014

[21] Oh, H.J., Lee, J.H., Kim, Y.J., Suh, S.J., Lee, J.H. and Chi, C.S. (2008) Surface Characteristics of Porous Anodic TiO_2 Layer for Biomedical Applications. *Materials Chemistry and Physics*, **109**, 10-14. http://dx.doi.org/10.1016/j.matchemphys.2007.11.022

[22] Das, K., Bandyopadhyay, A. and Bose, S. (2008) Biocompatibility and *in Situ* Growth of TiO_2 Nanotubes on Ti Using Different Electrolyte Chemistry. *Journal of the American Ceramic Society*, **91**, 2808-2814. http://dx.doi.org/10.1111/j.1551-2916.2008.02545.x

[23] Popat, K.C., Eltgroth, M., LaTempa, T.J., Grimes, C.A. and Desai, T.A. (2007) Decreased *Staphylococcus epidermis* Adhesion and Increased Osteoblast Functionality on Antibiotic-Loaded Titania Nanotubes. *Biomaterials*, **28**, 4880-4888. http://dx.doi.org/10.1016/j.biomaterials.2007.07.037

[24] Popat, K.C., Eltgroth, M., LaTempa, T.J., Grimes, C.A. and Desai, T.A. (2007) Titania Nanotubes: A Novel Platform for Drug-Eluting Coatings for Medical Implants? *Small*, **3/11**, 1878-1881. http://dx.doi.org/10.1002/smll.200700412

[25] Peng, L., Mendelsohn, A.D., LaTempa, T.J., Yoriya, S., Grimes, C.A. and Desai, T.A. (2009) Long-Term Small Molecule and Protein Elution from TiO_2 Nanotubes. *Nano Letters*, **9**, 1932-1936. http://dx.doi.org/10.1021/nl9001052

[26] Wang, Y., Feng, C., Jin, Z., Zhang, J., Yang, J.J. and Zhang, S.L. (2006) A Novel N-Doped TiO_2 with High Visible Light Photocatalytic Activity. *Journal of Molecular Catalysis A*: *Chemical*, **260**, 1-3. http://dx.doi.org/10.1016/j.molcata.2006.06.044

[27] Ghicov, A., Macak, J.M., Tsuchiya, H., Kunze, J., Haeublein, V., Frey, L. and Schmuki, P. (2006) Ion Implantation and Annealing for an Efficient N-Doping of TiO_2 Nanotubes. *Nano Letters*, **6**, 1080-1082. http://dx.doi.org/10.1021/nl0600979

[28] Ghicov, A., Macak, J.M., Tsuchiya, H., Kunze, J., Haeublein, V., Kleber, S. and Schmuki, P. (2006) TiO_2 Nanotube Layers: Dose Effects during Nitrogen Doping by Ion Implantation. *Chemical Physics Letters*, **419**, 426-429. http://dx.doi.org/10.1016/j.cplett.2005.11.102

[29] Shankar, K., Tep, K.C., Mor, G.K. and Grimes, C.A. (2006) An Electrochemical Strategy to Incorporate Nitrogen in Nanostructured TiO_2 Thin Films: Modification of Bandgap and Photoelectrochemical Properties. *Journal of Physics D*, **39**, 2361-2366. http://dx.doi.org/10.1088/0022-3727/39/11/008

[30] Li, Q. and Shang, J.K. (2009) Self-Organized Nitrogen and Fluorine Co-Doped Titanium Oxide Nanotube Arrays with Enhanced Visible Light Photocatalytic Performance. *Environmental Science and Technology*, **43**, 8923-8929. http://dx.doi.org/10.1021/es902214s

[31] Dong, L., Ma, Y., Wang, Y., Tian, Y., Ye, G., Jia, X. and Cao, G.X. (2009) Preparation and Characterization of Nitrogen-Doped Titania Nanotubes. *Materials Letters*, **63**, 1598-1600. http://dx.doi.org/10.1016/j.matlet.2009.04.022

[32] Xu, J., Ao, Y.H., Chen, M. and Fu, D. (2010) Photoelectrochemical Property and Photocatalytic Activity of N-Doped TiO_2 Nanotube Arrays. *Applied Surface Science*, **256**, 4397-4401. http://dx.doi.org/10.1016/j.apsusc.2010.02.037

[33] Park, J.H., Kim, S. and Bard, A.J. (2006) Novel Carbon-Doped TiO_2 Nanotube Arrays with High Aspect Ratios for Efficient Solar Water Splitting. *Nano Letters*, **6**, 24-28. http://dx.doi.org/10.1021/nl051807y

[34] Raja, K.S., Misra, M., Mahajan, V.K., Gandhi, T., Pillai, P. and Mohapatra, S.K. (2006) Photo-Electrochemical Hydrogen Generation Using Band-Gap Modified Nanotubular Titanium Oxide in Solar Light. *Journal of Power Sources*, **161**, 1450-1457. http://dx.doi.org/10.1016/j.jpowsour.2006.06.044

[35] Wu, G., Nishikawa, T., Ohtani, B. and Chen, A. (2007) Synthesis and Characterization of Carbon-Doped TiO_2 Nanostructures with Enhanced Visible Light Response. *Chemistry of Materials*, **19**, 4530-4537. http://dx.doi.org/10.1021/cm071244m

[36] Mohapatra, S.K., Misra, M., Mahajan, V.K. and Raja, K.S. (2007) Design of a Highly Efficient Photoelectrolytic Cell for Hydrogen Generation by Water Splitting: Application of $TiO_{2-x}C_x$ Nanotubes as a Photoanode and Pt/TiO_2 Nanotubes as a Cathode. *The Journal of Physical Chemistry C*, **111**, 8677-8685. http://dx.doi.org/10.1021/jp071906v

[37] Hahn, R., Ghicov, A., Salonen, J., Lehto, V.P. and Schmuki, P. (2007) Carbon Doping of Self-Organized TiO_2 Nano-

tube Layers by Thermal Acetylene Treatment. *Nanotechnology*, **18**, 105604 (pp4). http://dx.doi.org/10.1088/0957-4484/18/10/105604

[38] Lu, N., Zhao, H., Li, J., Quan, X. and Chen, S. (2008) Characterization of Boron-Doped TiO_2 Nanotube Arrays Prepared by Electrochemical Method and Its Visible Light Activity. *Separation and Purification Technology*, **62**, 668-673. http://dx.doi.org/10.1016/j.seppur.2008.03.021

[39] Su, Y., Han, S., Zhang, X., Chen, X. and Lei, L. (2008) Preparation and Visible-Light-Driven Photoelectrocatalytic Properties of Boron-Doped TiO_2 Nanotubes. *Materials Chemistry and Physics*, **110**, 239-246. http://dx.doi.org/10.1016/j.matchemphys.2008.01.036

[40] Yin, S., Yamaki, H., Komatsu, M., Zhang, Q., Wang, J., Tang, Q., Saito, F. and Sato, T. (2003) Preparation of Nitrogen-Doped Titania with High Visible Light Induced Photocatalytic Activity by Mechanochemical Reaction of Titania and Hexamethylenetetramine. *Journal of Material Chemistry*, **13**, 2996-3001. http://dx.doi.org/10.1039/b309217h

[41] Lu, N., Zhao, H., Li, J., Quan, X. and Chen, S. (2008) Characterization of Boron-Doped TiO_2 Nanotube Arrays Prepared by Electrochemical Method and Its Visible Light Activity. *Separation and Purification Technology*, **62**, 668-673.

[42] Vitiello, R.P., Macak, J.M., Ghicov, A., Tsuchiya, H., Dick, L.F.P. and Schmuki, P. (2006) N-Doping of Anodic TiO_2 Nanotubes Using Heat Treatment in Ammonia. *Electrochemistry Communications*, **8**, 544-548. http://dx.doi.org/10.1016/j.elecom.2006.01.023

[43] Macak, M., Ghicov, A., Hahn, R., Tsuchiya, H. and Schmuki, P. (2006) Photoelectrochemical Properties of N-Doped Self-Organized Titania Nanotube Layers with Different Thicknesses. *Journal of Materials Research*, **21**, 2824-2828. http://dx.doi.org/10.1557/jmr.2006.0344

[44] Lei, L., Su, Y., Zhou, M., Zhang, X.W. and Chen, X.Q. (2007) Fabrication of Multi-Non-Metal-Doped TiO_2 Nanotubes by Anodization in Mixed Acid Electrolyte. *Materials Research Bulletin*, **42**, 2230-2236. http://dx.doi.org/10.1016/j.materresbull.2007.01.001

[45] Tang, X.H. and Li, D.Y. (2008) Sulfur-Doped Highly Ordered TiO_2 Nanotubular Arrays with Visible Light Response. *Journal of Physical Chemistry C*, **112**, 5405-5409. http://dx.doi.org/10.1021/jp710468a

[46] Yang, X., Chen, J., Gong, L., Wu, M. and Yu, J.C. (2009) Cross-Medal Arrays of Ta-Doped Rutile Titania. *Journal of the American Chemical Society*, **131**, 12048-12049. http://dx.doi.org/10.1021/ja904337x

[47] Meng, F. (2005) Influence of Sintering Temperature on Semi-Conductivity and Nonlinear Electrical Properties of TiO_2-Based Varistor Ceramics. *Materials Science and Engineering B*, **117**, 77-80. http://dx.doi.org/10.1016/j.mseb.2004.10.021

[48] Feng, X., Shankar, K., Paulose, M. and Grimes, C.A. (2009) Tantalum-Doped Titanium Dioxide Nanowire Arrays for Dye-Sensitized Solar Cells with High Open-Circuit Voltage. *Angewandte Chemie*, **121**, 8239-8242. http://dx.doi.org/10.1002/ange.200903114

[49] Obata, K., Irie, H. and Hashimoto, K. (2007) Enhanced Photocatalytic Activities of Ta, N Co-Doped TiO_2 Thin Films under Visible Light. *Chemical Physics*, **339**, 124-132. http://dx.doi.org/10.1016/j.chemphys.2007.07.044

[50] Mura, F., Pozio, A., Masci, A. and Pasquali, M. (2009) Effect of a Galvanostatic Treatment on the Preparation of Highly Ordered TiO_2 Nanotubes. *Electrochimica Acta*, **54**, 3794-3798. http://dx.doi.org/10.1016/j.electacta.2009.01.073

[51] Dupuis, G. and Menu, M. (2006) Quantitative Characterisation of Pigment Mixtures Used in Art by Fibre-Optics Diffuse-Reflectance Spectroscopy. *Applied Physics A*, **83**, 469-474. http://dx.doi.org/10.1007/s00339-006-3522-3

[52] Simmons, E.L. (1975) Diffuse Reflectance Spectroscopy: A Comparison of the Theories. *Applied Optics*, **14**, 1380-1386. http://dx.doi.org/10.1364/AO.14.001380

[53] Yoldas, B.E. and Partlow, D.P. (1985) Formation of Broad Band Antireflective Coatings on Fused Silica for High Power Laser Applications. *Thin Solid Films*, **129**, 1-14. http://dx.doi.org/10.1016/0040-6090(85)90089-6

[54] Mor, G.K., Varghese, O.K., Paulose, M. and Grimes, C.A. (2005) Transparent Highly Ordered TiO_2 Nanotube Arrays via Anodization of Titanium Thin Films. *Advanced Functional Materials*, **15**, 1291-1296. http://dx.doi.org/10.1002/adfm.200500096

[55] Burgeth, G. and Kisch, H. (2002) Photocatalytic and Photoelectrochemical Properties of Titania-Chloroplatinate (IV). *Coordination Chemistry Reviews*, **230**, 41-47. http://dx.doi.org/10.1016/S0010-8545(02)00095-4

[56] Sakthivel, S. and Kisch, H. (2003) Daylight Photocatalysis by Carbon-Modified Titanium Dioxide. *Angewandte Chemie International Edition*, **42**, 4908-4911. http://dx.doi.org/10.1002/anie.200351577

[57] Lin, H., Huang, C.P., Li, W., Ni, C., Ismat Shah, S. and Tseng, Y. (2006) Size Dependency of Nanocrystalline TiO_2 on Its Optical Property and Photocatalytic Reactivity Exemplified by 2-Chlorophenol. *Applied Catalysis B*: *Environmental*, **68**, 1-11. http://dx.doi.org/10.1016/j.apcatb.2006.07.018

[58] Wei, W., Macak, J.M. and Schmuki, P. (2008) High Aspect Ratio Ordered Nanoporous Ta_2O_5 Films by Anodization of Ta. *Electrochemistry Communications*, **10**, 428-432. http://dx.doi.org/10.1016/j.elecom.2008.01.004

[59] Allam, N.K., Feng, X.J. and Grimes, C.A. (2008) Self-Assembled Fabrication of Vertically Oriented Ta_2O_5 Nanotube Arrays, and Membranes Thereof, by One-Step Tantalum Anodization. *Chemistry of Materials*, **20**, 6477-6481. http://dx.doi.org/10.1021/cm801472y

[60] Macak, J.M., Tsuchiya, H., Ghicov, A., Yasuda, K., Hahn, R., Bauer, S. and Schmuki, P. (2007) TiO_2 Nanotubes: Self-Organized Electrochemical Formation, Properties and Applications. *Current Opinion in Solid State and Materials Science*, **11**, 3-18. http://dx.doi.org/10.1016/j.cossms.2007.08.004

[61] Navale, S.C., Vadivel Murugan, A. and Ravi, V. (2007) Varistors Based on Ta-Doped TiO_2. *Ceramics International*, **33**, 301-303. http://dx.doi.org/10.1016/j.ceramint.2005.07.026

[62] Thamaphat, K., Limsuwan, P. and Ngotawornchai, B. (2008) Phase Characterization of TiO_2 Powder by XRD and TEM. *Kasetsart Journal*: *Natural Science*, **42**, 357-361. http://kasetsartjnatsci.kasetsart.org/

[63] Nashed, R., Szymanski, P., El-Sayed, M.A. and Allam, N.K. (2014) Self-Assembled Nanostructured Photoanodes with Staggered Bandgap for Efficient Solar Energy Conversion. *American Chemical Society Nano*, **8**, 4915-4923.

[64] Oliva, F.Y., Avalle, L.B., Santos, E. and Cámara, O.R. (2002) Photoelectrochemical Characterization of Nanocrystalline TiO_2 Films on Titanium Substrates. *Journal of Photochemistry and Photobiology A*: *Chemistry*, **146**, 175-188. http://dx.doi.org/10.1016/S1010-6030(01)00614-1

[65] Radecka, M., Rekas, M., Trenczek-Zajac, A. and Zakrzewska, K. (2008) Importance of the Band Gap Energy and Flat Band Potential for Application of Modified TiO_2 Photoanodes in Water Photolysis. *Journal of Power Sources*, **181**, 46-55. http://dx.doi.org/10.1016/j.jpowsour.2007.10.082

[66] van de Krol, R., Goossens, A. and Schoonman, J. (1997) Mott-Schottky Analysis of Nanometer-Scale Thin-Film Anatase TiO_2. *Journal of the Electrochemical Society*, **144**, 1723-1727. http://dx.doi.org/10.1149/1.1837668

[67] Bolts, J.M. and Wrighton, M.S. (1976) Correlation of Photocurrent-Voltage Curves with Flat-Band Potential for Stable Photoelectrodes for the Photoelectrolysis of Water. *The Journal of Physical Chemistry*, **80**, 2641-2645. http://dx.doi.org/10.1021/j100565a004

[68] O'Hayre, R., Nanu, M., Schoonman, J. and Goossens, A. (2007) Mott-Schottky and Charge-Transport Analysis of Nanoporous Titanium Dioxide Films in Air. *Journal of Physical Chemistry C*, **111**, 4809-4814. http://dx.doi.org/10.1021/jp068354l

[69] Bondarenko, A.S. and Ragoisha, G.A. (2005) Variable Mott-Schottky Plots Acquisition by Potentiodynamic Electrochemical Impedance Spectroscopy. *Journal of Solid State Electrochemistry*, **9**, 845-849. http://dx.doi.org/10.1007/s10008-005-0025-7

[70] Scharnweber, D., Beutner, R., Rössler, S. and Worch, H. (2002) Electrochemical Behavior of Titanium-Based Materials—Are There Relations to Biocompatibility? *Journal of Materials Science*: *Materials in Medicine*, **13**, 1215-1220. http://dx.doi.org/10.1023/A:1021118811893

[71] Jakob, M., Levanon, H. and Kamat, P.V. (2003) Charge Distribution between UV-Irradiated TiO_2 and Gold Nanoparticles: Determination of Shift in the Fermi Level. *Nano Letters*, **3**, 353-358. http://dx.doi.org/10.1021/nl0340071

Scientific Research Publishing (SCIRP) is one of the largest Open Access journal publishers. It is currently publishing more than 200 open access, online, peer-reviewed journals covering a wide range of academic disciplines. SCIRP serves the worldwide academic communities and contributes to the progress and application of science with its publication.

Other selected journals from SCIRP are listed as below. Submit your manuscript to us via either submit@scirp.org or Online Submission Portal.